Data-Driven Modelling for Predicting DBTT in Low-Alloy steels for Naval Application

M.Tech Thesis

By

SNEHUNGSU SAHANA

DEPARTMENT OF METALLURGICAL ENGINEERING AND MATERIALS SCIENCE (MEMS)

INDIAN INSTITUTE OF TECHNOLOGY INDORE

MAY 2025

Data-Driven Modelling for Predicting DBTT in Low-Alloy steels for Naval Application

A THESIS

Submitted in partial fulfillment of the
requirements for the award of the degree
of
Master of Technology

by
SNEHUNGSU SAHANA

DEPARTMENT OF METALLURGICAL ENGINEERING AND MATERIALS SCIENCE (MEMS)

INDIAN INSTITUTE OF TECHNOLOGY INDORE

MAY 2025

INDIAN INSTITUTE OF TECHNOLOGY INDORE

CANDIDATE'S DECLARATION

I hereby certify that the work which is being presented in the thesis entitled **Data-Driven Modelling for Predicting DBTT in Low-Alloy steels for Naval Application** in the partial fulfillment of the requirements for the award of the degree of **MASTER OF TECHNOLOGY** and submitted in the **DEPARTMENT OF METALLURGICAL ENGINEERING AND MATERIALS SCIENCE, Indian Institute of Technology Indore**, is an authentic record of my own work carried out during the time period from July 2023 to May 2025 under the supervision of **Dr. Chandan Halder, Assistant Professor, IIT Indore.**

The matter presented in this thesis has not been submitted by me for the award of any other degree of this or any other institute.

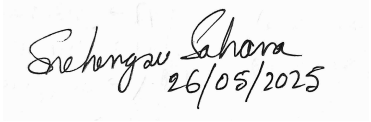

Signature of the student with date
(SNEHUNGSU SAHANA)

This is to certify that the above statement made by the candidate is correct to the best of my knowledg

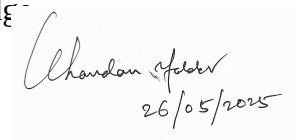

Signature of the Supervisor of
M.Tech. thesis (with date)
(Dr. Chandan Halder)

SNEHUNGSU SAHANA has successfully given his M.Tech. Oral Examination held on **May 22, 2025**.

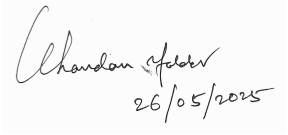

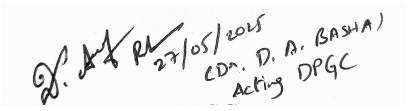

Signature of Supervisor of M.Tech. thesis
Date:

Convener, DPGC
Date:

ACKNOWLEDGEMENTS

I would like to express my deepest gratitude to Dr. Chandan Halder Sir, my supervisor at IIT Indore, for his invaluable guidance, encouragement, and support throughout the course of my M.Tech thesis. His expertise and mentorship have been instrumental in shaping this work.

I am equally grateful to Dr. Abhijit Ghosh, for his mentorship and insightful suggestions during the project. His experience and advice have greatly enriched my research.

I would also like to extend my heartfelt thanks to Dr. Bashista Kumar Mahanta sir, Senior project associate, Indian Institute of Petroleum CSIR, Dehradun and Praveen Kumar Sir who is a research scholar from my lab for his assistance and constructive feedback, which played a significant role in the successful completion of this thesis.

Finally, I am grateful to my family, friends, and colleagues for their constant encouragement and understanding throughout this journey.

Thank you all for being a part of this endeavor.

Abstract

Ductile-to-brittle transition temperature (DBTT) is an important material property for ascertaining the structure integrity and reliability of naval steel, particularly under low-temperature and high-strain-rate conditions experienced in maritime conditions. Lower DBTT provides greater fracture resistance and minimizes the probability of disastrous brittle failure, rendering it an important naval performance parameter. Conventional strategies for optimizing DBTT are based significantly on experimental protocols and empirical models, which are frequently time-consuming, expensive, and not very scalable. To meet these demands, the current work investigates a data-driven approach employing machine learning (ML) methods for prediction and optimization of the DBTT curve in naval steels, thus streamlining material design and performance analysis.

The work starts from the acquisition and preparation of a detailed dataset including compositional data, microstructural and thermodynamic descriptors (e.g., grain size, phase fractions, and dislocation energy), and mechanical properties obtained both experimentally and by thermodynamic calculations. The central aim of the project is to reduce the DBTT while increasing the Upper Self Energy—a measure of a material's resistance to deformation and defect creation. These two targets were chosen because they were most relevant to impact toughness as well as structural behavior under dynamic loading conditions.

Several machine learning algorithms, such as regression and multi-objective optimization methods, were used to model the non-linear relations between input variables and target characteristics. Feature extraction and data normalization were also carried out to enhance model robustness and explainability. The optimization process utilized non-dominated sorting and Pareto front analysis for trade-off analysis among conflicting objectives, where in this case, combinations where DBTT would be minimized without affecting or lowering the Upper Self Energy significantly were emphasized.

Interestingly, in all eight feature combinations and optimization situations, the outcome unanimously showed an inverse, positive relationship between Transition Temperature and Upper Self Energy. That is, with any rise in Upper

Self Energy, there was a corresponding increase in DBTT, contrary to the original design requirement. This implies an inherent correlation between the two goals, ostensibly due to the microstructural response of the material—e.g., phase distribution, dislocation interactions, and thermodynamic stability. It is saying that mechanisms that build up higher energy absorption capability or resistance in the microstructure also increase the transition temperature, indicative of a compromise that cannot be ignored.

This led to a closer examination of model behavior and feature contributions. It was discovered that some alloying elements and microstructural characteristics exerted a dual effect, stimulating stability but, unintentionally, increasing DBTT. The research highlights the value of choosing input variables that facilitate greater decoupling of target properties, or the design of more advanced ML models with the ability to manage such trade-offs better.

In summary, This project showcases how machine learning can help improve key material properties like DBTT and USE in naval steels. While there were some initial hurdles, the study uncovered meaningful patterns between mechanical and thermodynamic behavior. Most importantly, the final optimized model outperformed the best experimental data, achieving a lower DBTT and higher USE. These results highlight the real potential of combining machine learning with materials engineering to accelerate smarter and more focused material development.

TABLE OF CONTENTS

LIST OF FIGURES

LIST OF TABLES

NOMENCLATURE

DBTT: Ductile to Brittle Transition Temperature

USE: Upper Self Energy

LSE: Lower Self Energy

HSLA Steels: High Strength Low Alloy steels

CVN: Charpy V-Notch

MAE: Mean Absolute Error

RMSE: Root Mean Square Error

EvoNN: Evolutionary Neural Network

EvoDN: Evolutionary Deep Neural Network

cRVEA: constrained Reference Vector Guided Evolutionary Algorithm

NSGA: Non-dominated Sorting Genetic Algorithm

Chapter 1

Introduction

- Low-alloy steels, particularly high-strength low-alloy (HSLA) steels, are notable for their strength, toughness, and resistance to harsh marine environments, which makes them crucial for the construction of naval vessels and infrastructure. Understanding and accurately predicting the DBTT is vital because it determines the temperature range within which these materials can maintain their mechanical integrity under operational stresses, particularly under the low-temperature conditions typically encountered at sea [1][2][3]. The significance of DBTT in naval applications arises from the need for materials that can endure extreme conditions without failure. As naval technology continues to evolve, optimizing the DBTT of these materials has become increasingly important for enhancing safety and structural reliability.

Traditionally, the DBTT has been determined using experimental methods, such as the Charpy impact test, which measures the toughness of a material by recording the energy absorbed during fracture at various temperatures. A transition curve was plotted by testing multiple samples across different temperature ranges. However in recent years, data-driven modeling has been increasingly applied to improve decision-making and predictive power by utilizing complex, high-volume operational data. It is the use of sophisticated computational methods and machine learning algorithms to predict the ductile–brittle transition temperature (DBTT) in low-alloy steels. Recent advancements in data-driven modelling have transformed the traditional methods of predicting DBTT by employing machine-learning techniques that analyze vast datasets to uncover patterns and correlations that influence material behavior. These innovative methodologies enable researchers to simulate various conditions and predict the DBTT with improved accuracy compared to conventional experimental approaches [4]. However, challenges such as data quality issues, skilled personnel shortages complicate the widespread adoption of these models in real-world applications [5][6]. The ongoing exploration of data-driven modelling techniques highlights their potential not only in predicting DBTT but also in refining the understanding of the complex interrelations among chemical

composition, processing parameters, and mechanical performance in low-alloy steels. [7][8] As this field progresses, the integration of improved data collection and analysis methods promises to enhance the reliability of predictive models, ultimately contributing to the development of safer and more effective naval structures.[9][10].

1.1 Low-Alloy steels :- Low-alloy steels play a critical role in various structural applications, particularly in the naval industry, owing to their favorable mechanical properties and performance characteristics. High-strength low-alloy (HSLA) steels, for instance, are widely employed in the construction of bridges, ship hulls, and mining equipment, benefiting from their strength and toughness under extreme conditions.

In naval applications, there is a pressing need for materials that offer exceptional combinations of yield strength, low-temperature impact toughness, ductility, ballistic resistance, and weldability [2]. The Ongoing investigations of their properties and potential applications continue to shape the future of naval engineering.

These steels typically incorporate different alloying elements that are designed to achieve specific microstructures .The chemical composition of these steels is carefully tailored to achieve these properties. The base metal is iron (Fe), with carbon content typically in the range of 0.10 to 0.20 wt%. The relatively low carbon content helps ensure good weldability while still contributing to strength through the formation of martensite. Manganese (0.70–1.60%) is included to enhance strength and toughness, while nickel (1.5–3.5%) significantly improves toughness and corrosion resistance. Chromium (0.3–1.0%) adds to corrosion and oxidation resistance, and molybdenum (0.1–0.5%) increases hardenability and high-temperature strength. Silicon (0.2–0.5%) acts as a deoxidizer and also contributes slightly to strength. Impurities such as phosphorus and sulfur are kept to very low levels (typically less than 0.02%) to avoid embrittlement and ensure good toughness and ductility. [11] A notable aspect of HSLA steels is their carbon equivalent (CE), which is often greater than 0.50. Although a higher CE can enhance certain properties, it negatively influences the weldability of the material, thereby posing challenges during fabrication. [12]

The microstructure of low-alloy steels is crucial because it significantly affects their mechanical properties. It is typically dominated by tempered martensite, which is produced through quenching followed by tempering heat treatment. This structure provides high strength while maintaining good toughness and ductility. In some cases, especially with variations in cooling rates and compositions, bainite may also be present, further contributing to toughness. Ferrite and pearlite are generally minimized or absent in quenched and tempered steels but may appear in normalized grades. Fine precipitates of carbides, such as Fe_3C or Mo_2C, can form during tempering and help to further strengthen the steel matrix [13].

1.2 DBTT (Ductile to Brittle Transition Temperature) :- The Ductile to Brittle Transition Temperature (DBTT) is a critical parameter in the evaluation of the toughness of steel, particularly in low-alloy steels used for naval applications. The DBTT is defined as the temperature at which a material changes its behavior from being ductile (can bend or stretch without breaking) to brittle (breaks suddenly without much bending). Above the DBTT, materials can absorb more energy before breaking. Below it, they break more easily and without warning. For many steels, including low carbon steels, the DBTT is approximately -75°C

Several factors influence DBTT, including the chemical composition, grain size, heat treatment, and overall microstructure of the material [14,15]. The presence of specific alloying elements can significantly alter the DBTT. For instance, elements such as manganese and nickel have been shown to lower DBTT and enhance toughness, whereas higher concentrations of carbon, phosphorus, sulfur, and oxygen increase DBTT [16]. Processing parameters such as Slabsoak temperature, Finish Rolling temperature, Grain size, Carbide thickness significantly influences the DBTT. For instance, Higher soak temperatures can lead to grain coarsening, which, upon cooling, results in larger ferrite grains. Larger grains are associated with higher DBTT, making the steel more susceptible to brittle fracture at lower temperatures. Rolling at lower temperatures, particularly in the non-recrystallization region, promotes the

formation of finer grains through mechanisms like dynamic recrystallization. Finer grains enhance toughness and lower the DBTT. According to the Hall-Petch relationship, finer grains impede crack propagation, enhancing toughness and reducing DBTT. Studies have shown that refining ferrite grain size from 40 μm to 2 μm can decrease the DBTT from approximately 0°C to –220°C. This significant reduction underscores the importance of grain refinement in improving low-temperature toughness [17].Thinner, finely dispersed carbides can enhance toughness by impeding crack initiation and propagation. In contrast, thicker carbides can act as stress concentrators, facilitating crack initiation and increasing the DBTT. [18]

The measurement of the DBTT is essential for ensuring the safety and reliability of structural materials. In recent advances data-driven modeling have introduced machine-learning techniques for predicting DBTT through training on experimentally extracted features. For stable evaluation, the data is divided into training and test sets and cross-validation is used to avoid overfitting. Feature extraction and standardization are preceded by Principal Component Analysis (PCA) for dimensionality reduction. Models like Random Forest Regressor (RFR), Linear Regression (LIN), and K-Means Clustering (KMC) are trained on principal components. RFR is additionally optimized by nested cross-validation, and LIN is a baseline model. Model performance is measured on validation scores indicating bias and variance, and an ensemble of RFR models is employed to enhance prediction robustness on the test set [19].

Experimental data are utilized in machine learning models to forecast ductile-to-brittle transition temperature (DBTT). Six algorithms for regression, namely linear regression (LR), SMOReg, K-nearest neighbors (KNN), random forest (RF), multi-layer perceptron (MP), and random committee (RC), are trained and tested on the basis of statistical measures such as Pearson correlation coefficient (PCC), coefficient of determination (R^2), mean absolute error (MAE), and root mean squared error (RMSE). Ten-fold cross-validation is performed to improve the robustness of the model and prevent overfitting [20]. Understanding and optimizing DBTT is paramount in the context of naval applications because of the unique environmental conditions faced by these materials.

1.3 Data driven modeling techniques:- Data-driven modeling plays a crucial role in enhancing forecasts in fields such as materials science. Through the application of large datasets, it clarifies how materials respond when subjected to various conditions. With enhanced data gathering and processing power, modeling has transitioned to involve greater emphasis on modeling actual data, thereby making more intelligent and accurate decisions [12, 21].

Data-driven approaches include the use of machine learning algorithms to identify trends in large data sets and can predict the future behavior of materials from present data streams and enable optimization and improved understanding of properties like the ductile-to-brittle transition temperature (DBTT) in low-alloy steels, especially naval applications [22, 23].

To efficiently harness data-driven methodology, there must be a clear preprocessing and analyzing of gathered information. Methods that include data normalization, extraction of features, and using statistics are essential steps to validate precision and appropriateness in predicting models. It isolates effects of particular variables and makes forecasting more reliable through controlling for the confounding influences. The incorporation of machine learning into data-driven modelling allows for more sophisticated analysis and the development of better predictive systems. Machine learning techniques can manage large amounts of structured and unstructured data, which makes it possible to find intricate patterns and relationships that may be overlooked by conventional techniques. This integration is especially useful for applications such as materials property evaluation, where there are various interacting variables that determine outcomes.[21]

Chapter 2

Literature Review

2.1 Importance of DBTT in Structural and Naval Usage

The Ductile-to-Brittle Transition Temperature (DBTT) is a key mechanical property in structural materials, particularly steel in naval environments. This temperature marks the transition point where a material transforms from ductile fracture (energy-absorbing) to brittle fracture (catastrophic failure). Naval steels are commonly exposed to severe conditions such as sub-zero temperatures and high-impact loads, thus the knowledge and optimization of DBTT are vital for structural integrity and safety.

Traditional methods for DBTT assessment are based on experimental methods like the Charpy V-Notch (CVN) test. These methods are time-consuming, sample preparation sensitive, and frequently incapable of extrapolating results over different compositions and histories. In addition, naval steels commonly possess complex, functionally graded microstructures that develop during processing, rendering characterization of DBTT using physical testing only more challenging.

2.2 DBTT Influencing Factors in Steels

A number of metallurgical factors control DBTT, such as grain size, alloying content, types of microstructure, and conditions of processing. Grain refinement has always been found to decrease DBTT by inhibiting crack growth, while coarse grains are linked with an increased DBTT. The occurrence of ferrite-pearlite, martensite, or bainite structures profoundly influences fracture modes and transition behavior.

In steels with ultrafine grain sizes or cementite/ferrite bimodal grain structures, effective grain size becomes a crucial concept. Instead of average grain size, the largest cleavage unit size—is determined by crystallographic and boundary orientation—controls crack propagation. Hence, microstructural engineering that leads to beneficial cleavage path changes is critical for attaining beneficial DBTT values.

Also, alloying additions such as Ni, Cr, Mo, and B are employed in designing DBTT behavior. Nickel, for instance, enhances toughness without substantially impacting strength, of particular concern for naval use at low temperatures. The issue occurs when these elemental additions couple non-linearly with mechanical properties, creating a multi-variable problem in optimizing DBTT.

2.3 Machine Learning Role in DBTT Prediction

Machine Learning (ML) provides a potential path to DBTT prediction and optimization through the creation of data-based surrogate models. Such models are able to resolve intricate, non-linear relationships between input parameters (e.g., composition, microstructure descriptors, and processing conditions) and DBTT outputs.

Some of the commonly used ML algorithms are Linear Regression, Random Forest, k-Nearest Neighbors, Multi-layer Perceptrons, Genetic Programming (GP), and Minimax Probability Machine Regression (MPMR). These methods have shown robust performances in DBTT prediction using experimental and simulated datasets as learning datasets.

Notably, ML models can be constructed to deal with high-dimensional input spaces with limited data using feature engineering, dimensionality reduction, and symbolic regression. Model prediction interpretation is facilitated using techniques such as SHAP (SHapley Additive exPlanations), hence providing insight into which features most significantly impact DBTT. This is especially useful for microstructural or compositional levers' identification, which can be optimized during alloy design or thermomechanical processing.

2.4 Feature Engineering and Dimensionality Reduction

One of the major issues in using ML for DBTT prediction is input feature high dimensionality and correlation. The input features are elemental concentrations, physical atomic properties (e.g., ionization energy, cohesive energy), and thermodynamic parameters. Weakly correlated or redundant features can decrease model performance and result in overfitting.

In order to counteract this, hybrid feature selection methods are utilized that blend correlation-based filtering with algorithms such as F-score ranking or recursive feature elimination. These methods isolate the physically most relevant descriptors, including cohesive energy and ionization energy, which were found to correlate highly with DBTT in numerous intermetallic and steel systems.

Employing just a subset of carefully chosen features not only enhances model interpretability and diminishes the computational expense, but also leads to better generalization to new steel grades or unobserved processing conditions. The achieved low-dimensional models can map input parameters to DBTT efficiently and serve as the foundation for process optimization and tuning of alloys.

2.5 Model Validations and Performance Assessment

The dependability of machine learning models for DBTT prediction relies on strict validation processes. Typical practices are k-fold cross-validation, split testing, and external validation through independent datasets. Model accuracy is measured using performance measures like R^2, MAE (Mean Absolute Error), RMSE (Root Mean Square Error), and PCC (Pearson Correlation Coefficient).

In more thorough analyses, graphical methods such as Taylor diagrams and Regression Error Characteristic (REC) plots are employed to represent prediction confidence in multiple statistical spaces. Models with high accuracy but low complexity are the ones most favored for implementation in material design pipelines.

Of the models, Genetic Programming (GP) has been noted for its potential to extract symbolic expressions representing relationships between DBTT and input variables with both predictive ability and physical meaningfulness. In the same vein, emotional neural networks (ENN) and MPMR approaches have been considered for their distinct learning methods, adding more to viable DBTT modeling.

2.6 Implications for Naval Steel Optimization

In naval steels, where performance and safety under harsh conditions are of utmost priority, the capability to forecast and tune DBTT with the help of ML is of critical importance. Data-driven models can be utilized to simulate alloy composition and microstructures virtually and avoid expensive and time-consuming experiments.

In addition, coupling ML with material informatics and heat treatment databases allows for inverse design: from a desired DBTT, optimum alloy compositions and heat treatment routes can be suggested. This is especially useful to develop functionally graded steels (FGS) or multiphase steels designed specifically for impact resistance below zero degrees.

In prospective applications, ML-improved frameworks may be integrated into digital replicas of steel production lines, where in-process monitoring and real-time DBTT prediction are possible with the help of sensor data. This integration fills the void between laboratory-scale materials science and industrial implementation, enabling the creation of next-generation naval steels with enhanced toughness profiles.

2.7 DBTT Sensitivity to Irradiation and Heat Treatment

DBTT is extremely sensitive to irradiation, particularly for ferritic/martensitic steels employed in nuclear and maritime environments. These steels undergo marked embrittlement upon neutron irradiation, leading to a remarkable upward shift in DBTT. This is important for naval steel service, where irradiation can arise from proximity to nuclear propulsion equipment or high-energy weapon impact situations.

Studies have proven that irradiation-induced hardening and embrittlement in steels can be suppressed by controlled heat treatment processes and selective impurity doping. For example, tempering at subtly elevated temperatures (for example, 780 °C compared to 750 °C) and optimizing holding times minimize DBTT shift following irradiation. These processes improve carbide distribution uniformity and minimize residual stress, making toughness post-irradiation better.

In addition, the effects of impurity additions like boron (B) and nitrogen (N) have been identified to be critical. Isotopically pure boron additions (e.g., ^11B) and small amounts of nitrogen decrease DBTT shift significantly when used together with optimized heat treatments. This is due to their capacity to alter precipitate chemistry, retard boron segregation in the grain boundaries, and enhance beneficial microstructures that are resistant to irradiation damage. These results highlight the necessity of combining alloy chemistry and processing history in predictive models. Machine learning architectures can leverage this metadata to predict DBTT shifts in service conditions, facilitating design and selection of steel for radiation-resistance applications.

2.8 Microstructural Mechanisms of DBTT and Fracture

Microstructurally, initiation and extension of brittle fracture in steels in the DBTT regime are governed by dislocation-precipitate interactions. In carbide-rich reduced activation ferritic/martensitic (RAFM) steels, candidate materials for fusion and naval reactor use, carbide shape and composition play a critical role in influencing crack formation.

Experimental investigations with Focused Ion Beam (FIB) and Transmission Electron Microscopy (TEM) proved that Cr-rich ellipsoidal carbides are preferred sites for nucleation of brittle cracks. They are larger in size and elongated, in contrast to smaller spherical iron-rich carbides. The composition and shape of these precipitates promote dislocation pile-ups and site concentration of local stresses at the carbide-matrix interface, ultimately causing decohesion and crack initiation. Whereas smaller and rounder carbides do not really hinder dislocation movement and thereby, have less to contribute to stress concentration. The tendency for crack development in certain microstructural regions can then be directly correlated with carbide type, shape, and distribution.

In machine learning applications, descriptors like carbide size distribution, phase fractions, precipitate morphology, and grain boundary character can be added to predict DBTT behavior. High-resolution imaging can be quantified into features through image processing pipelines and applied to supervised ML models to predict DBTT or fracture toughness.

2.9 Machine Learning Integration with Irradiation Effects

A sophisticated topic of DBTT prediction involves modeling irradiation-induced microstructural changes effects using data-driven methodology. Since irradiation changes mechanical properties and fracture behavior with time, time-dependent and irradiation-dependent variables must be addressed by any ML model. Through the integration of irradiated steel experimental data sets, ML algorithms can acquire the intricate correlation between irradiation dose (dpa), helium generation, impurity levels, heat treatment procedures, and shifts in DBTT. The models may also include irradiation hardening measures, such as yield strength or hardness variations, as intermediate predictors.

Experiments have revealed that helium atoms generated upon irradiation can also be responsible for intensified DBTT shifts. Quantification of the relationship between helium content (in ppm) and DBTT shift is possible and can be incorporated into predictive models as a component of multi-objective optimization strategies, where both toughness preservation and radiation resistance can be addressed concurrently.

2.10 Toward Predictive Design of Radiation-Resistant Naval Steels

The integrated knowledge of metallurgical research and AI modeling accentuates the capability of hybrid optimization solutions for DBTT. Under such systems, physical metallurgy is used to direct feature selection, whereas machine learning models carry out the optimization and prediction processes.

For marine use, this equates to the fact that engineers are able to now model how a steel alloy would behave in a spectrum of operating temperatures and irradiation levels without physically testing each permutation of conditions. This expedites the materials development process, makes it less expensive, and improves the dependability of naval vessels.

For instance, an ML model learned on DBTT behavior in RAFM steels with attributes such as carbide morphology, irradiation dose, alloying

composition, and heat treatment schedule would anticipate the optimal steel composition for submarine hulls to minimize embrittlement throughout life.

Although a lot of work has been done on the ductile-to-brittle transition temperature (DBTT) behavior in naval steels, such that most studies are based on conventional empirical or experimental approaches, recent publications have attempted to investigate the application of machine learning (ML) for predicting materials properties. There is still limited work directed toward the optimization of the DBTT curve for naval steels through ML. Additionally, combining microstructural characteristics, processing conditions, and composition in a single predictive model remains an under investigated area. This identifies an imperfection, which calls for a data-driven strategy built upon machine learning to not only predict but also optimize the DBTT response for improved performance in naval systems. [25, 26, 27, 28]

Chapter 3

Methodolgy

3.1 Dataset: In this study, we proposed two distinct strategies of training in combination with two different optimization techniques for investigating the DBTT of the low alloy naval steels. Both the training strategies involves the utilization of the dataset as input variables containing alloy compositions like silicon [Si], Sulphur [S], Phosphorus [P], Manganese [Mn], Nubium [Nb], Alumunium [Al], Carbon [C] and rest is Iron [Fe], different processing parameters like Slabsoak Temperature, Finish Rolling Temperature [FRT], Reduction Ratio [RR], Carbide Thickness [t*]), Grain Size [d], Pearlite Grain Size [Pe], Cooling Rate [CR] and Four output variables like Temperature corresponding to 27 Joule Impact Energy (^{o}C), Temperature corresponding to 54 Joule Impact Energy (^{o}C), Ductile to Brittle Transition Temperature (^{o}C), Upper Self Energy (Joule).

	Processing parameters							**Percentage Weight Fraction**						
	Slabsoak	FRT	RR	t*	d	Pe	CR	Si	S	P	Mn	Nb	Al	C
Range	**1140 - 1300**	**725 - 889**	**2 - 4**	**0.21 - 0.38**	**5.03 - 10.06**	**10.0 - 17.5**	**7.80 - 31.2**	**0.156 - 0.392**	**0.008 - 0.016**	**0.015 - 0.029**	**0.88 - 1.50**	**0.017 - 0.047**	**0.004 - 0.056**	**0.08 - 0.14**
Unit	**^{O}C**	**^{O}C**	**-**	**µm**	**µm**	**µm**	**^{O}C/min**	**wt%**	**wt%**	**wt%**	**wt%**	**wt%**	**wt%**	**wt%**

Table 1: Processing parameters and alloying elements ranges.

Slab soak temperature, finish rolling temperature, and cooling temperature, all impact the microstructure of steel, which in turn impacts the ductile-to-brittle transition temperature (DBTT). Increasing slab soak and finish rolling temperatures encourage grain refinement, while controlled cooling (for example, accelerated cooling) facilitates the development of tougher phases such as bainite, both contributing to reduced DBTT and enhanced toughness [29, 30]. Reduction ratio, thickness of carbide, and thickness of pearlite are all very closely related to each other and collectively determine the ductile-to-

brittle transition temperature (DBTT) of steel. An increase in reduction ratio while rolling refines the pearlitic structure and can reduce the thickness of the carbide layers, which generally enhances toughness and reduces the DBTT. Nevertheless, if lamellae of carbide or pearlite become too thick, they can be sites for crack initiation, which raises the DBTT. Hence, accurate regulation of deformation and microstructural characteristics is required to optimize low-temperature toughness. Larger grain sizes reduce toughness and raise the ductile-to-brittle transition temperature (DBTT), making the material more susceptible to brittle fracture [31, 32] .

The general impact of alloying elements like carbon, silicon, manganese, sulfur, phosphorus, niobium, and aluminum on ductile-to-brittle transition temperature (DBTT) in steel is due to their sum effect on microstructure. Increased content of carbon leads to greater strength but may favor brittle phases as well as the DBTT increase. Sulfur and phosphorus, even in minute quantities, separate at grain boundaries and play an important role in embrittlement, thereby increasing the DBTT. Manganese counteracts the undesirable effects of sulfur by the formation of manganese sulfides and also assists in grain structure refinement, overall enhancing toughness and reducing the DBTT. Silicon, while serving as a deoxidizer, possesses a mild embrittling influence if its quantity is high. Niobium and aluminum play a beneficial role by precipitating as fine precipitates that restrain grain growth, resulting in grain refinement that enhances low-temperature toughness and lowers DBTT. Thus, the DBTT of a steel is not determined by one element but by the synergistic interaction of all these elements and their influence on grain size and the existence of brittle phases [33, 34]. Although the individual effect of each parameter is known, their combined effect remains unclear. Therefore, we aim to identify potential correlations among all the parameters.

3.2 <u>Modification in Dataset</u>: Based on this dataset to increase the accuracy of the training and to reduce the complexity of the model two different approaches have been taken. First, is the “Normalization” of the dataset. Our dataset has high variance in feature values—for example, slab soak temperature ranges from 1140 to 1300 °C, whereas alloying element concentrations have small

decimal range, and the temperatures corresponding to 27 and 54 Joules of impact energy are negative. So, normalization achieves the goal that all features will be reduced to a comparable magnitude (0 to 1), which achieves faster convergence in the model as well as protects features with enormous numerical ranges to not dominate learning. The formula is shown below,

$$norm(x) = \frac{x - min(x)}{max(x) - min(x)}$$

Here, x_{norm} represents the normalized value, min(x) & max(x) represents the minimum value and maximum value of each individual input.

In addition to normalizing the experimental dataset, another approach was adopted to improve the results—using the carbon equivalent in place of several individual elemental inputs. Employing the carbon equivalent (CE) value rather than considering separate alloying elements has an important benefit: it gives one simple, combined measure of the general hardenability and weldability of a steel by taking into consideration the overall effect of more than one element (such as C, Mn, Si, Cr, Ni, Mo, etc.). This enables engineers to rapidly determine how a steel will act when heat-treated or cooled Without having to figure out the complex interactions of each element one by one. The conversion rule is shown below,

CEV (%) = %C + %Si/30 + (%Mn + %Cu + %Cr)/20 + %Ni/60 + %Mo/15 + %V/10 + 5(%B)

Among all these elements enlisted in the formula our dataset consists of only Silicon and Manganese except carbon. So the relation reduces to only **[%C + %Si/30 + %Mn/20],** and the number of independent columns has been reduced to 13 from 15. Both training and optimization were performed on each of the datasets.

3.3 <u>Machine Learning strategies</u>: Data-driven modeling to optimize the ductile-to-brittle transition temperature (DBTT) is a process of applying machine learning methods to identify intricate relationships between composition, processing parameters, and DBTT. The process begins with preprocessing and training, in which models like linear regression, support vector machines (SVM), decision trees are used for preprocessing purposes and neural networks are used to train on experimental or industrial data. Such models train patterns in terms of error reduction between anticipated and real DBTT values using typical optimization routines like single or multi-objective Gradient-based optimization, Probabilistic or model-based Bayesian optimization or multi-objective Evolutionary optimization like Reference Vector-guided Evolutionary Algorithm (RVEA) and Non-dominated Sorting Genetic Algorithm (NSGA) for adjusting parameters within models. The goal is to develop a predictive model capable of not only accurately estimating DBTT but also assisting in determining the critical influencing factors and their optimal combination to get the best possible optimum results. Trained and validated, these models enable material design and process control through predicting DBTT from input variables without requiring comprehensive physical testing.

For our problem we have adopted two different training approaches Evolutionary Neural Networks (EvoNN) & Evolutionary Deep Neural Network 2 (EvoDN2), because they use evolutionary methods to automatically create and optimize neural networks, allowing them to find the best structure and settings while balancing different goals like accuracy and simplicity for better overall performance and two different optimization processes Constrained Reference Vector-guided Evolutionary Algorithm (cRVEA) & Non-dominated Sorting Genetic Algorithm - II (NSGA-II), because we need to optimize three objective simultaneously. So, this makes 4 combinations on 2 datasets comprising 8 models altogether.

EvoNN, or Evolutionary Neural Network, is a machine learning paradigm that integrates the concepts of evolutionary algorithms and neural networks to optimize the structure as well as the weights of the model. In contrast to conventional neural networks that depend only on gradient-based training

techniques such as backpropagation, EvoNN employs evolutionary techniques like genetic algorithms to iteratively evolve a population of neural networks. Every network is scored according to a fitness function that generally regards accuracy of prediction and occasionally model complexity. New generations of neural networks are generated through selection, crossover, and mutation, enabling the algorithm to venture into a larger and more varied set of solutions. This method makes it possible to find network configurations that are potentially more optimal, particularly for complicated or nonlinear problems where conventional training may not perform well. EvoNN is especially useful in applications where model interpretability, architecture search, or resistance to local minima are crucial. [34]

Whereas, EvoDN2 (Evolutionary Deep Neural Network 2) is a sophisticated machine learning algorithm that builds on the strength of EvoNN (Evolutionary Neural Network) by supporting deeper structures and more advanced optimization methods. While EvoNN concentrates on developing neural network topologies and weights through evolutionary algorithms, EvoDN2 builds on this by incorporating deep learning methods for the ability to model more intricate, nonlinear patterns in data. It utilizes multi-objective optimization algorithms such as the constrained Reference Vector-guided Evolutionary Algorithm (cRVEA). This allows EvoDN2 to optimize multiple conflicting objectives at the same time, e.g., minimizing prediction error and model complexity. In addition, EvoDN2's design facilitates the inclusion of domain-specific constraints and goals, enabling a more specialized and efficient modeling method for complicated systems. [33]

Now comes the optimization part, optimization is the process of fine-tuning model parameters (such as weights in a neural network) to reduce a loss function and enhance prediction accuracy. It is generally performed during training rather than before or after, as training itself is an optimization procedure—repeatedly refining the model to best match the data. Without it, the model would not learn useful patterns from the dataset. The Constrained Reference Vector-guided Evolutionary Algorithm (cRVEA) is a special extension of the standard Reference Vector-guided Evolutionary Algorithm (RVEA) for solving constrained multi-objective optimization problems. RVEA emphasizes

diversity and convergence in the objective space with reference vectors but does not consider constraints and assumes that all candidate solutions are feasible. On the other hand, cRVEA involves a constraint-handling strategy that prefers feasible solutions and punishes constraint violations and is thus better suited to real-world problems where constraints are typically strict and unavoidable. The algorithm guides a population of candidate solutions towards well-distributed Pareto-optimal fronts by partitioning the objective space using reference vectors to preserve diversity. In selection, the people are selected on the basis of both how close they are to these vectors and how well constrained they are. Offspring are created with crossover and mutation by using the fittest individuals, and constraint-handling methods ensure that infeasible solutions either get penalized or rejected. This integration of feasibility in the selection step allows cRVEA to optimally trade off between optimality and satisfaction of constraints and hence is specially useful for high-level tasks such as model tuning, where the objectives such as accuracy and simplicity need to be optimized together within given constraints. [28]

On the other hand NSGA-II (Non-dominated Sorting Genetic Algorithm II) is a sophisticated evolutionary multi-objective optimization algorithm for addressing problems that have conflicting objectives. It employs non-dominated sorting to assign ranks to solutions, separating the population into various fronts according to dominance, and uses a crowding distance factor to ensure diversity in the population. It also includes elitism, which ensures that the best solutions obtained are passed to the next generation, avoiding loss of good-quality solutions. The crowding distance approach in NSGA-II also increases diversity by choosing solutions that are well-separated in the objective space and hence provide a more spread Pareto front. NSGA-II offers better convergence, diversity, and computational efficiency with a time complexity of O(MNlogN), and hence it is more efficient for complex optimization tasks. [39]. Our final plot is not like a usual Pareto plot since, rather than with two competing objectives, we have three. In order to simplify matters, the condition for selecting non-dominated solutions was not incorporated into our algorithm. The non-dominated outputs are then filtered manually at a later point.

3.4 Heatmap: Heatmap is a graphical tool that displays data values by variations in color. It provides an immediate and clear means of displaying complicated data sets, facilitating the identification of patterns, trends, and outliers without the need to concentrate on individual numerical values. Our dataset contains 14 independent variables and 4 dependent variables as described before. To understand how each input parameter is correlated with the outputs the heatmap of the correlation matrix is plotted. The values of the correlation matrix are determined via a statistical indicator known as the Pearson correlation coefficient (r) [31]. It measures the linear relationship between two variables, say X and Y. The formula is,

$$\mathbf{r = Cov\,(X,Y) \,/\, (\sigma_X \,.\, \sigma_Y)}$$

Where,

Cov(X,Y) is the covariance between X & Y, i.e how they vary together.
σ_X and σ_Y are the standard deviations of X & Y.

(+1) value in the correlation matrix indicates a perfect positive linear correlation (Dark red colour), meaning both variables increase together. A value of (0) signifies no linear relationship between the variables (Lighter or neutral colours), while a coefficient of (–1) represents a perfect negative linear relationship (Dark blue colour), where one variable increases as the other decreases. The correlation heatmap for my experimental dataset is shown in the results section in Fig 2.

3.5 Equation for DBTT plot: To analyze the ductile-to-brittle transition behavior more accurately, because analyzing only the values doesn't provide as clear an understanding as looking at the entire plot, so the temperature-dependent results were curve-fitted by the hyperbolic tangent function:

$$E(T) = A + B\ tanh\left(\frac{T - T0}{d}\right)$$

In this equation, E(T) is the measured property, like impact energy or fracture toughness, as a function of temperature. The parameter A is the midpoint between the upper and lower shelf values ((Upper Self Energy + Lower Self Energy) / 2) and controls the vertical location of the curve. The parameter B is half the difference between the upper and lower shelf values ((Upper Self

Energy - Lower Self Energy) / 2) and determines the range of the transition. The transition temperature, T_0, is defined as the inflection point at which the rate of change in mechanical behavior is largest. Lastly, the parameter C determines the steepness of the transition; smaller values of C correspond to a sharper transition, whereas larger values correspond to a more gradual change.

Fitting the equation to the data enables a smooth and continuous characterization of the ductile-to-brittle transition, which is impossible using discrete data point analysis by itself. The technique permits a better determination of the transition temperature and presents a clearer picture of how the material behavior changes from ductile to brittle. In this work, the fitted curves closely followed the experimental data for different temperature ranges, showing the effectiveness of the model in representing both the position and sharpness of the transition. Moreover, the extracted parameters provide useful information for comparing materials or checking model predictions, hence enhancing the robustness of both scientific interpretation and practical application. The Experimental DBTT plots are shown in Fig 1,

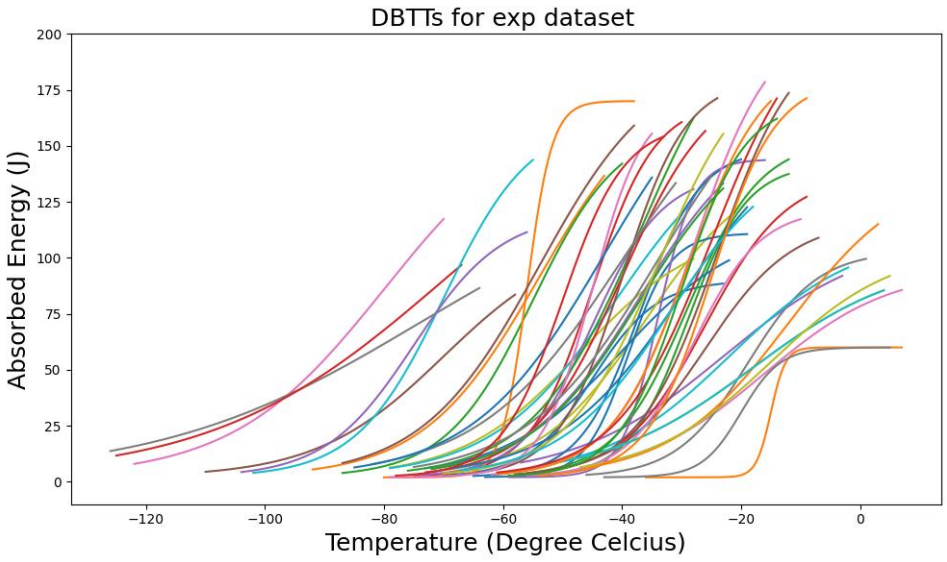

Fig 1: Experimental DBTT plots

Chapter 4

Results & Discussions

4.1 Correlation matrix: In order to understand the correlation of the outputs with the inputs i.e how each output varies with each individual inputs the heatmap is analyzed. The correlation heatmap for my experimental dataset is like following,

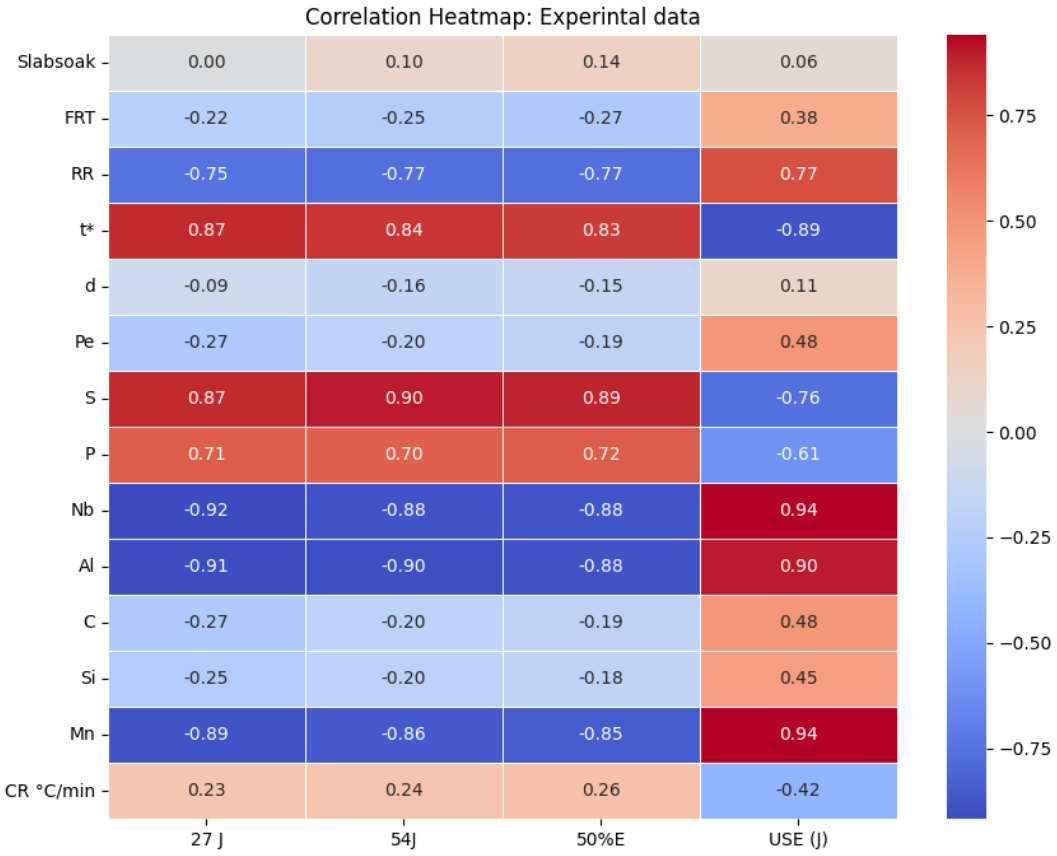

Fig 2: correlation heatmap for the experimental dataset

The correlation matrix shows a high positive correlation (0.94) between Manganese content and Upper Self Energy, which means that an increase in Manganese weight percentage has a positive relationship with an increase in Upper Self Energy. However, Carbide Thickness is highly negatively correlated (-0.89) with Upper Self Energy, and this implies that when carbide thickness increases, Upper Self Energy decreases. The relationship between Grain Size and Upper Self Energy is fairly low (0.11), suggesting only a very weak positive correlation.

It can be seen from the heatmap visualization that Reduction Ratio, Niobium, Aluminum, and Manganese have high negative correlations with the

temperatures of 27 Joules, 54 Joules, the transition temperature, and with Upper Self Energy. By contrast, Carbide Thickness, Sulfur, and Phosphorus have high positive correlations with the temperatures and negative correlations with Upper Self Energy.

4.2 Accuracy of the model: Since this is literature-based data rather than experimental data, there are no outliers present. Therefore, an error versus complexity plot is not necessary, and only the model fittings are presented. A minimal gap must exist between training and validation accuracy, which shows good generalization to new data. Validation accuracy must be high and consistent, affirming the model's goodness on unseen data. Also, the lack of overfitting (where training accuracy is significantly greater than validation accuracy) and underfitting (where both training loss and validation loss are low) indicates that the model learned well and training and validation curves must look smooth, indicating stable and effective learning during training. In order to inspect the accuracy of our trained model for the Normalized dataset (having 14 inputs (7 processing parameters and 7 compositions) and 3 outputs (27 Joule temperature, 54 Joule temperature, Upper Self Energy)), a fitting process was utilized on the predicted values using the least squares method with an objective to find the best parameters in order to optimize the DBTT and the Upper Self Energy of the system. Two models Evolutionary Neural Network & Evolutionary Deep Neural Network were used for training purposes. The fitting was done by the least squares approach, in which the model parameters were optimized to reduce the difference between the predicted and observed values. Between two models employed, EvoDN2 provides better outcomes so, the fitting results for EvoDN2 alone are presented here, the fitting gave a coefficient of determination (R^2) value of average 0.97 for all of the three objectives, reflecting a high correlation between the experimental data and the fitted model. This indicates that 97% of the variance in the data is explained by the model, which is consistent with the expectation of high precision for such studies.

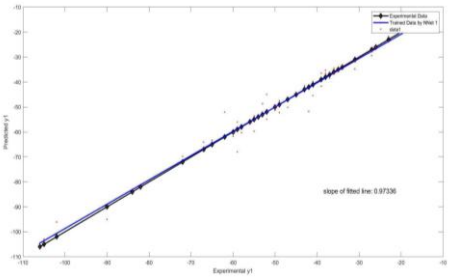

Fig 3(c)

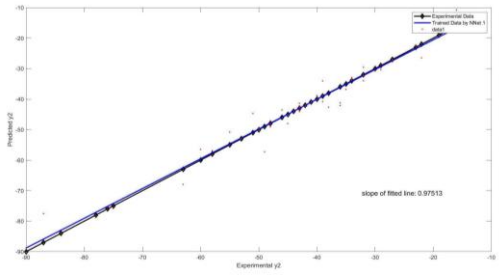

Fig 3(b)

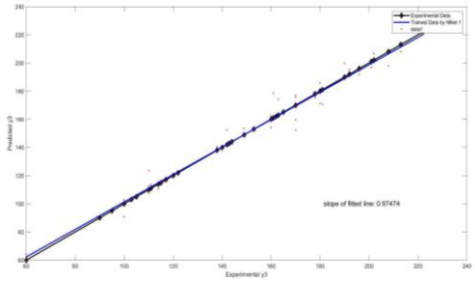

Fig 3(c)

Fig 3: Fitting for Y1 (Fig 3(a)) with R^2 value 0.97336, Fitting for Y2 (Fig 3(b)) with R^2 value 0.97513, Fitting for Y3 (Fig 3(c)) with R^2 value 0.97474

Figure 2 shows the fitting results for each of the three objectives. The model matches the experimental data well, showing that it is accurate enough for the planned analysis and predictions.

4.3 <u>Distribution of the predicted outputs</u>: The distribution of the predicted outputs needs to be examined to determine how well the model is doing across the whole dataset. This enables us to visualize whether the predictions are consistent and reliable, and whether the model has a propensity to make some kinds of error, such as predicting too high or too low in some places. By looking at the spread of the predicted values, we can determine whether the model is biased or whether it generalizes well to various input conditions. Looking at the distribution also provides information regarding how the output varies with inputs, which comes in handy to understand the nature of the model more thoroughly. Distribution of the predicted inputs and the predicted outputs are shown in 2D plots and 3D plot respectively in Fig 4. All input variables exhibited a uniform distribution across the entire range, indicating that all of them are equally important and none can be excluded from the analysis for our optimization task.

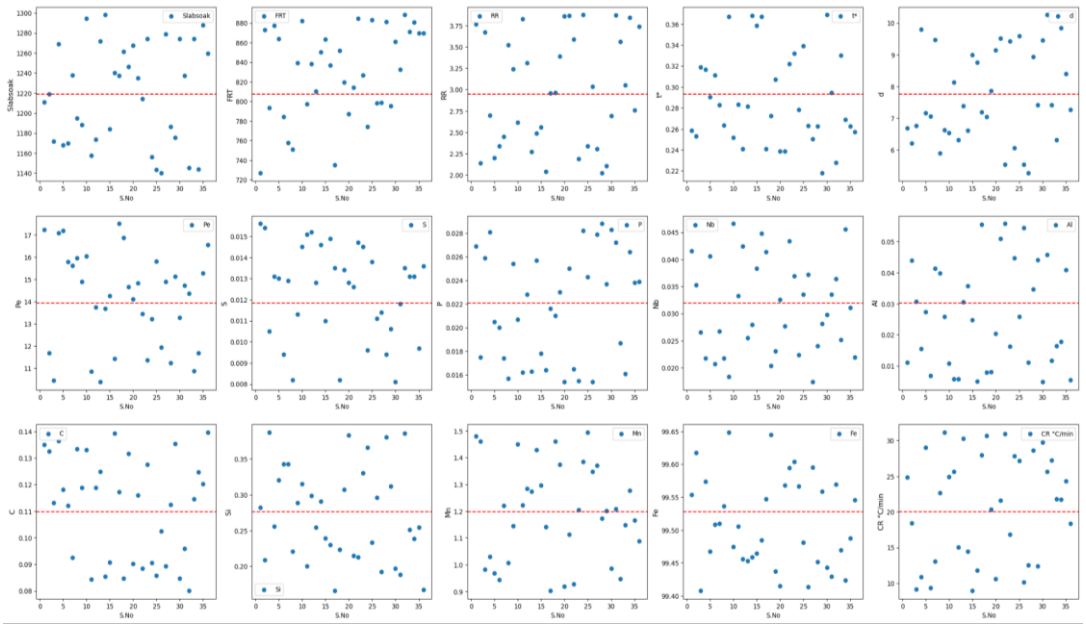

Fig 4(a)

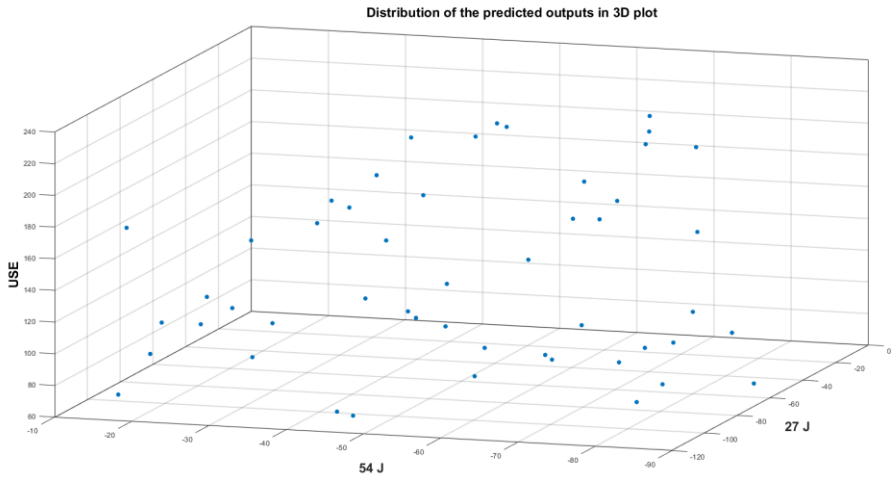

Fig 4(b)

Fig 4: Distribution of 35 predicted inputs (Fig 4(a)), distribution of 35 predicted outputs (Fig 4(b))

4.4 <u>Comparison of slopes</u>: A comparison of predicted and experimental curve slopes assists in determining if the model correctly describes the rate of change of the DBTT. There are cases where the predicted DBTT may match experimental data, but a mismatch in slope can signal improper modeling of transition sharpness or toughness variation at the DBTT. This comparison is significant for both comprehending the inherent fracture mechanisms and guaranteeing stable material performance in engineering applications.

Therefore, it is compared three slopes representing various transition temperature ranges, and the outcome suggests that our model is adequately trained and successfully captures the overall slope trend throughout these regions. The plots are shown below Fig 5.

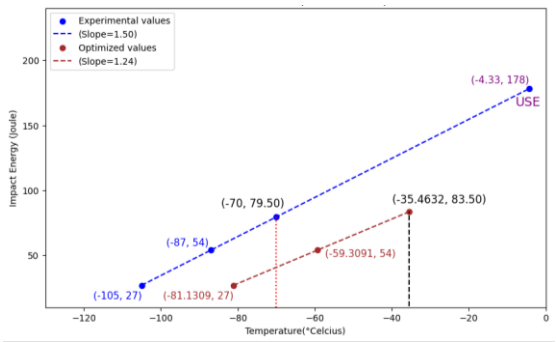

Fig 5(a)

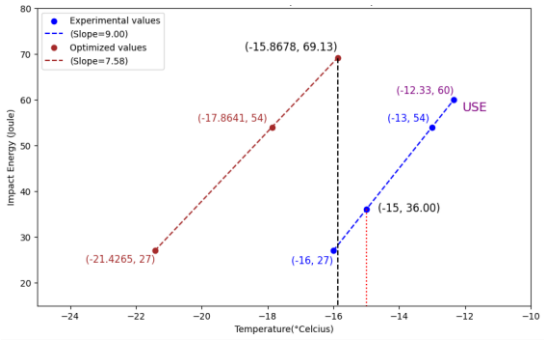

Fig 5(b)

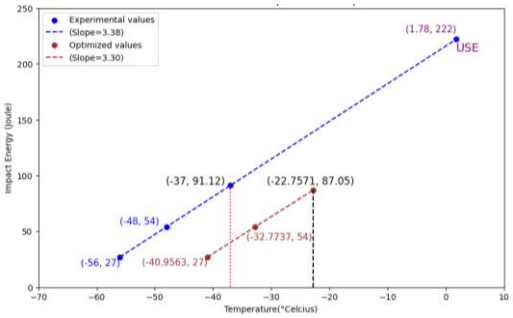

Fig 5(c)

Fig 5: Comparison of slopes for different DBTT ranges

In all of the above three plots the Blue line represents the Experimental values and the red line indicates the predicted values. All of the above plots show a similar trend with the respective experimental values.

4.5 <u>Predicted DBTT plots</u>: The predicted values from all combinations fall within the range of the experimental dataset, as shown in Fig 6,

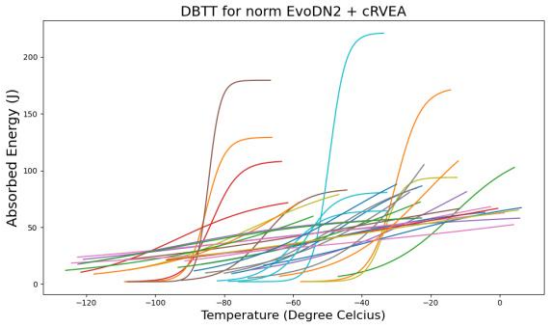

Fig 6(a)

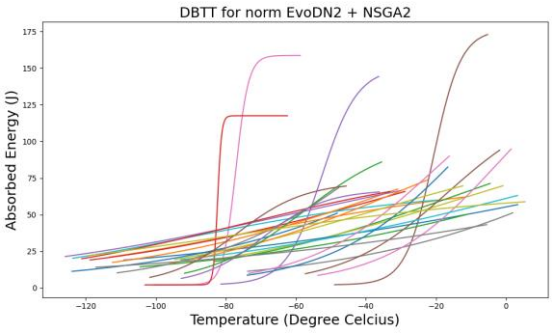

Fig 6(b)

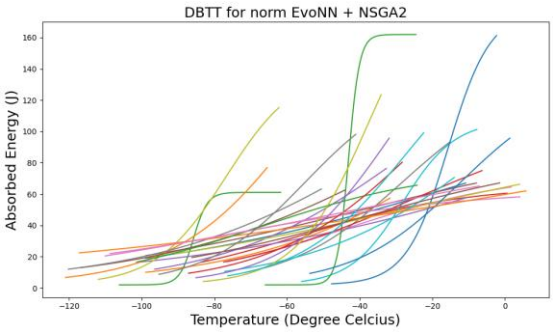

Fig 6(c)

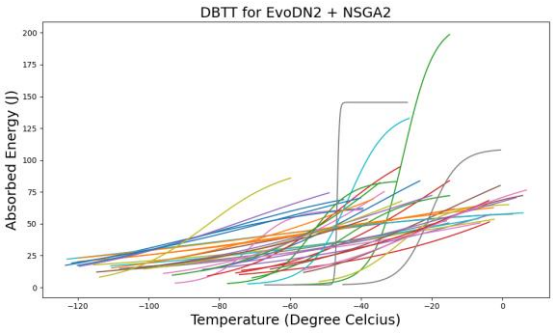

Fig 6(d)

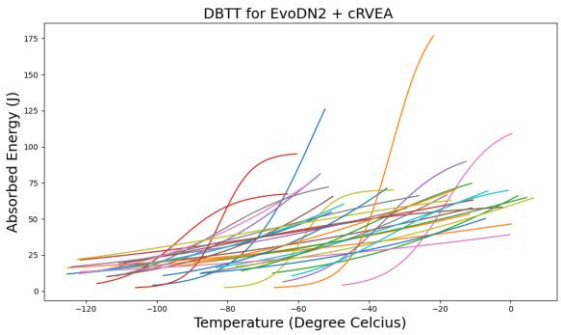

Fig 6(e)

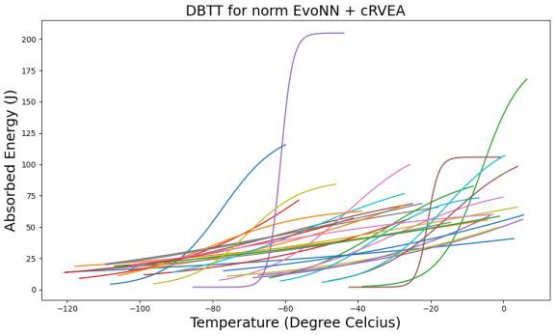

Fig 6(f)

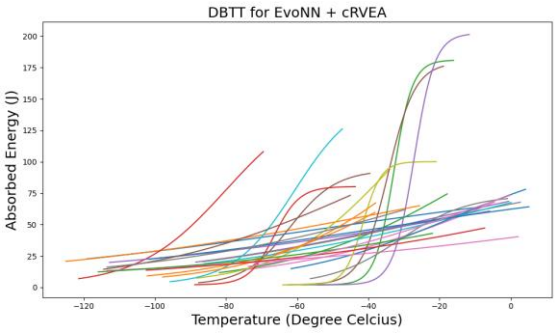

Fig 6(g)

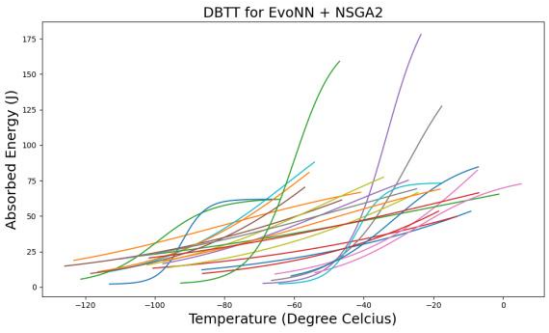

Fig 6(h)

4.6 <u>Non-Dominated plots</u>: Working with all the predicted plots is really hectic that's why instead of analyzing all, only non-dominated plots have been considered. In our problem, the non-dominated graph for the three-objective optimization—to maximize Upper Shelf Energy (USE) while minimizing the Ductile-to-Brittle Transition Temperature (DBTT)—plots a trade-off surface on which these two goals are naturally competing. While DBTT drops (a better leftward shift), USE drops (undesirable), and thus cannot both be optimized together without compromise. The non-dominated front is a collection of best trade-off solutions in which any improvement in reducing DBTT comes at the expense of some reduction of USE, and vice versa. Understanding this front is important as it identifies the best that can be achieved under this dilemma, allowing balanced material performance to be selected intelligently. The non-dominated plots are shown in Fig 7,

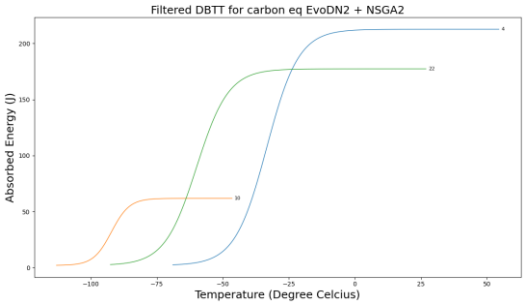

Fig 7(a)

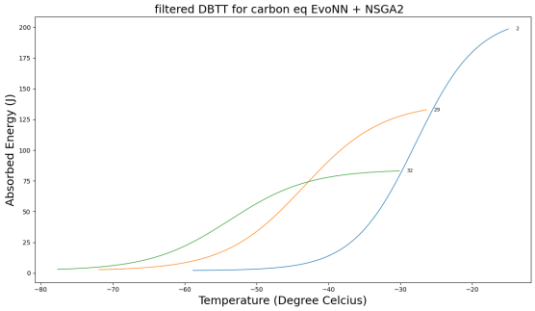

Fig 7(b)

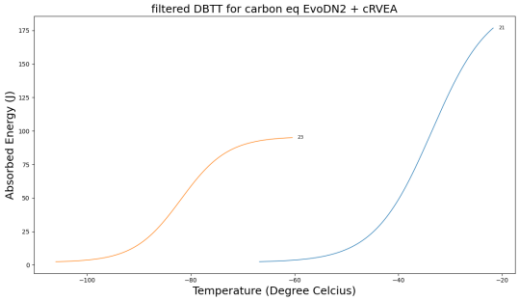

Fig 7(c)

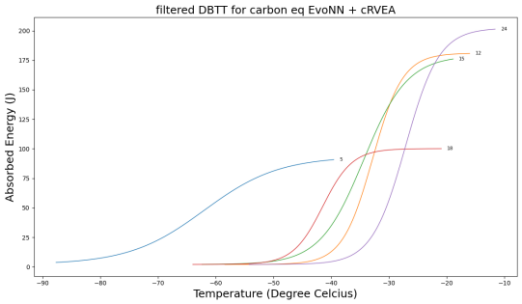

Fig 7(d)

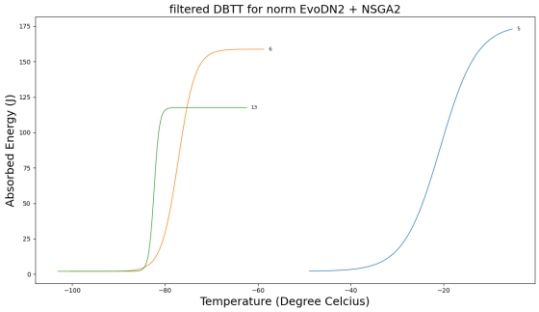

Fig 7(e)

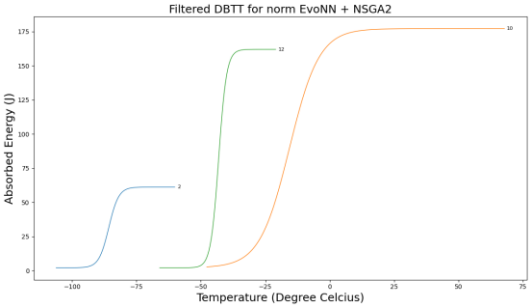

Fig 7(f)

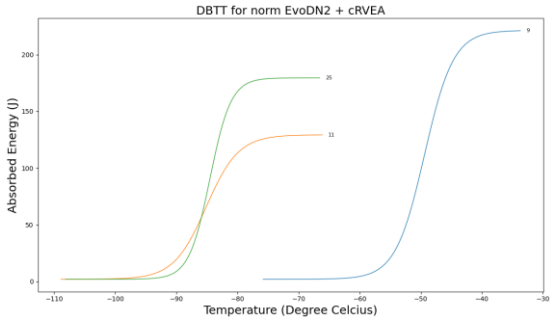

Fig 7(g)

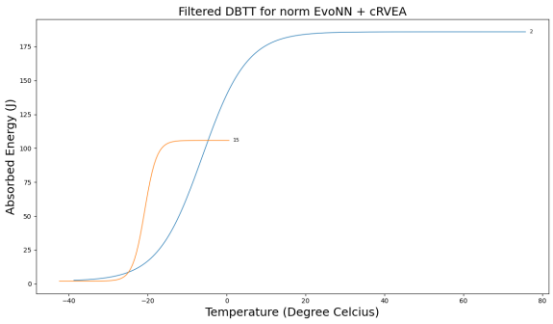

Fig 7(h)

Fig 7: Non-dominated DBTT plots

The trend noticed in the non-dominated plots, wherein Upper Self Energy and Transition Temperature rise together in all eight combinations, implies a correlated relationship between these two objectives. The ideal was to reduce the Transition Temperature (for enhanced toughness) while providing for an upward rise in Upper Self Energy, which in general implies a stable microstructure. But the simultaneous increase in both parameters suggests that there is a trade-off that might be caused by underlying compositional or microstructural limitations. The correlation might also be intrinsic material behavior—whereby factors that are responsible for energy absorption (e.g., higher dislocation density or phase stability) tend to increase the DBTT as well. The ML model may also be picking out prominent features that have a positive effect on both parameters, thereby preventing an examination of what are contradictory improvements. These results highlight the necessity of optimizing the feature set, using more stringent constraints, or seeking out other ML architectures that can more effectively capture nonlinear decoupling between the goals.

Analyses and Discussion

- To gain a better insight into the causes of the trends determined for the ductile-to-brittle transition temperature (DBTT), a comparison was made between two DBTT plots: one based on experimental data and one from predictive modeling. Though both shared similar general trends, the predicted plot showed better upper shelf energy and lower DBTT, reflecting better toughness and ductility. Four sets of comparisons have been made, for EvoDN2 training (since EvoDN2 was trained better for our study compared to EvoNN), all individual comparison plots are shown in Fig 8 along with tables (Table 2(a) - Table 2(d))

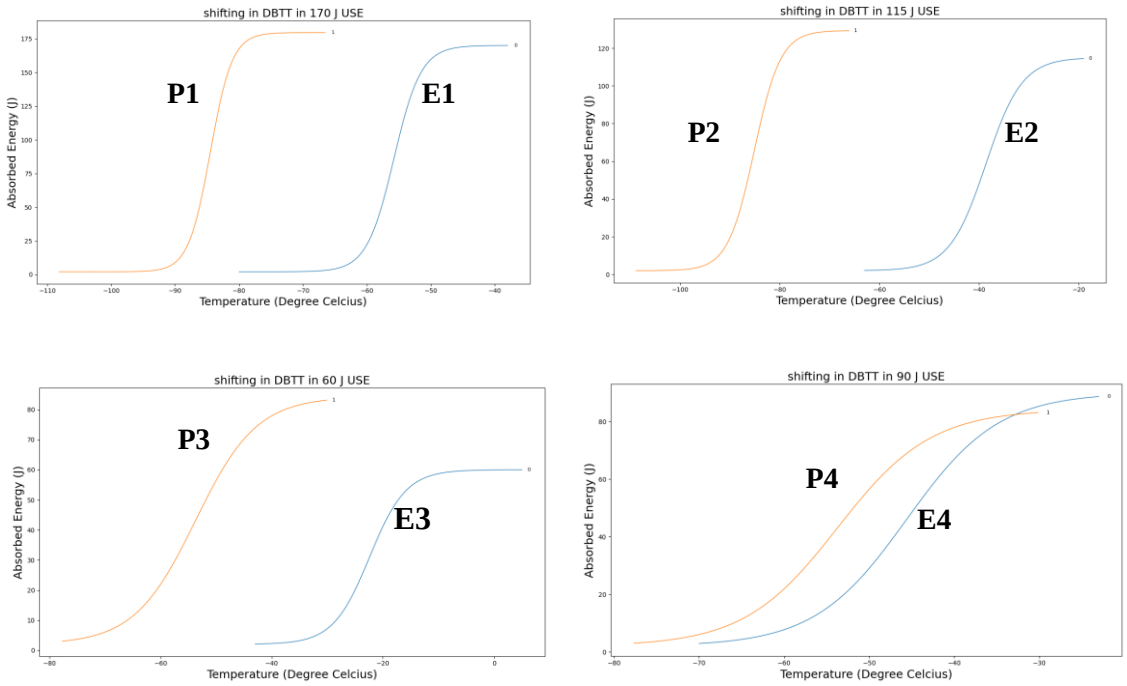

Fig 8 : Comparison of predicted plots and experimental plots

For each input parameter, a rigorous evaluation was made to establish its particular impact on the DBTT response. From this investigation, robust conclusions were possible for some of the main parameters. A thorough examination of these findings is covered in the following section. Tabular overviews of the results for all four parameters are summarized below.The first row of Table 2(a) corresponds to plot E1, while the second row corresponds to P1. Similarly, the first row of Table 2(b) corresponds to plot E2, and the second

to P2. Table 2(c) and Table 2(d) follow the same pattern, with their first and second rows referring to plots E3,P3 and E4,P4, respectively. Tables 2(a) and 2(b) present a comparison of results obtained without using the carbon equivalent dataset, whereas Tables 2(c) and 2(d) compare results derived from the carbon equivalent dataset.

Slabsoak	FRT	RR	t*	d	Pe	S	P	Nb	Al	C	Si	Mn	CR	27 J	54J	50% E	USE
1140	760	3.2	0.303	7.932	13.75	0.009	0.029	0.031	0.036	0.110	0.392	1.3	9.75	-60.00	-58.00	-56.00	170.00
1230.179	790	2.5	0.234	6.890	16.94	0.010	0.018	0.025	0.032	0.106	0.359	1.0	21.9	-88.13	-86.54	-84.49	179.51

Table 2(a)

Slabsoak	FRT	RR	t*	d	Pe	S	P	Nb	Al	C	Si	Mn	CR	27 J	54J	50% E	USE
1220	826	3.2	0.314	7.688	10	0.008	0.020	0.035	0.008	0.080	0.266	1.21	13.0	-43.00	-39.00	-39.00	115.00
1257.255	865	2.8	0.319	5.038	12.83	0.013	0.017	0.033	0.010	0.101	0.275	1.09	11.8	-88.86	-86.11	-85.12	129.33

Table 2(b)

Slabsoak	FRT	RR	t*	d	Pe	S	P	Nb	Al	C_eq	CR	27 J	54J	50% E	USE
1220	808	2	0.378	7.334	17.5	0.016	0.029	0.022	0.018	0.194	13.0	-23.00	-15.000	-20.000	60.000
1287.418	810	3.1	0.319	6.397	18.26	0.015	0.017	0.046	0.009	0.170	18.6	-57.66	-50.114	-53.712	84.230

Table 2(c)

Slabsoak	FRT	RR	t*	d	Pe	S	P	Nb	Al	C_eq	CR	27 J	54J	50% E	USE
1200	814	4	0.378	10.02	10	0.009	0.023	0.017	0.005	0.131	15.6	-50.00	-43.000	-45.000	90.000
1287.418	810	3.1	0.319	6.397	18.26	0.015	0.017	0.046	0.009	0.170	18.6	-57.66	-50.114	-53.712	84.230

Table 2(d)

Table 2: 2(a) shows the comparison of USE 170 J and 180 J, 2 (b) shows comparison of USE 115 J and 129 J, 2(c) shows the comparison of USE 60 J and 84 J, 2(d) shows the comparison of USE 90 J and 84 J

Chapter 5

Conclusions

On the basis of the four separate comparisons carried out, a merged evaluation was also done. While the limited variation in some elements made it hard to spot consistent trends, a few showed a clear connection with DBTT and USE, which helped support their individual influence. These insights led to some key conclusions, and the optimal value was identified through the analysis. The conclusions are listed below:

(i) The dataset is successfully trained and modelled and the optimization process successfully carried out.

(ii) It was concluded after individually analyzing all the input parameters that the Slab Soak Temperature, Pearlite Size, and Cooling Rate should be high; the Carbide Thickness should be in the mid-range; and the Reduction Ratio should lie between the mid to high range. Here, 'high' and 'low' refer to the upper and lower bounds of each input parameter as defined in Table 1.

(iii) The best outcome achieved among all the predicted results, is a USE of 179.51 Joules and a DBTT of -84.49 °C, which surpasses the best experimental result in terms of both metrics. The best experimental result shows a USE of 170 Joules and a DBTT of -56.00 °C. For the input parameters corresponding to the optimized result, please refer to P1 in Table 2.

REFERENCES

1 W. J. Liu, H. Y. Li, Y. J. Kong, J. W. Liu, D. Liu, Q. Gao, N. Q. Peng and X. J. Xiong, *J Cent South Univ*, 2025, 32, 776–788.

2 R. Cheng, Y. Jin, M. Olhofer and B. Sendhoff, *IEEE Transactions on Evolutionary Computation*, 2016, 20, 773–791.

3 B. Guo, L. Fan, Q. Wang, Z. Fu, Q. Wang and F. Zhang, *Metals (Basel)*, DOI:10.3390/met6120323.

4 Y. Zhang, D. Zou, X. Wang, F. Xia, Y. Wang and W. Zhang, *Metals and Materials International*, 2022, 28, 1630–1638.

5 B. K. Mahanta and N. Chakraborti, *Computer Methods in Material Science*, DOI:10.7494/cmms.2021.3.0733.

6 C. D. Yang, Y. Liu, G. Y. Zhou, X. L. Zou, X. G. Lu and G. H. Cao, *Materials*, DOI:10.3390/ma15238405.

7 A. Kabanov, G. Korpala, R. Kawalla and U. Prahl, *Steel Res Int*, DOI:10.1002/srin.201800336.

8 H. Rahmanifard and I. Gates, *Artif Intell Rev*, DOI:10.1007/s10462-024-10865-5.

9 D. Zhu, K. Pan, H. H. Wu, Y. Wu, J. Xiong, X. S. Yang, Y. Ren, H. Yu, S. Wei and T. Lookman, *Journal of Materials Research and Technology*, 2023, 26, 8836–8845.

10 I. Matetić, I. Štajduhar, I. Wolf and S. Ljubic, *MDPI*, 2023, preprint, DOI: 10.3390/s23010001.

11 V. Nasir and F. Sassani, *Springer Science and Business Media Deutschland GmbH*, 2021, preprint, DOI: 10.1007/s00170-021-07325-7.

12 Y. Li, J. Zhao, X. Li, Z. Xing, Q. Duan, X. Liang and X. Wang, *Journal of Materials Research and Technology*, 2024, 33, 6494–6507.

13 J. Clauß, L. Caetano and Å. Bror Svinndal, *Energy Build*, DOI:10.1016/j.enbuild.2024.114310.

14 F. Kiehas, M. Reiter, J. P. Torres, M. Jerabek and Z. Major, *Front Mater*, DOI:10.3389/fmats.2023.1275640.

15 E. Sadeghpour and A. Nonn, *Comput Mater Sci*, DOI:10.1016/j.commatsci.2022.111782.

16 A. Moitra, A. Das Gupta, S. Sathyanarayanan, G. Sasikala, S. K. Albert, S. Saroja, A. K. Bhaduri, E. R. Kumar and T. Jayakumar, in *Procedia Engineering*, Elsevier Ltd, 2014, vol. 86, pp. 258–263.

17 P. Karagiannidis and N. Themelis, *Ocean Engineering*, DOI:10.1016/j.oceaneng.2021.108616.

18

19 X. Xie, J. Bennett, S. Saha, Y. Lu, J. Cao, W. K. Liu and Z. Gan, *NPJ Comput Mater*, DOI:10.1038/s41524-021-00555-z.

20 K. Anjali, S. N. Yesilyurt, P. Samui, H. Y. Dalkilic and O. M. Katipoglu, *Civil Engineering Infrastructures Journal*, 2024, 57, 189–203.

21 X. Wang, *Title Page Integrated Computational Materials Design for Alloy Additive Manufacturing: Introducing Data-Driven Approach to Physical Metallurgy*, 2023.

22 C. Frie, A. Kolyshkin and C. Eberl, *Fatigue Fract Eng Mater Struct*, 2024, 47, 1036–1052.

23 C. Shang, D. Zhu, H. H. Wu, P. Bai, F. Hou, J. Li, S. Wang, G. Wu, J. Gao, X. Zhou, T. Lookman and X. Mao, *Scr Mater*, DOI:10.1016/j.scriptamat.2024.116023.

24 *Chapter 3 Multiple Linear Regression Model The linear model*, .

25 B. Shabash and K. C. Wiese, in *GECCO 2018 Companion - Proceedings of the 2018 Genetic and Evolutionary Computation Conference Companion*, Association for Computing Machinery, Inc, 2018, pp. 1449–1456.

26 M. S. Bingley, *Effect of grain size and carbide thickness on impact transition temperature of low carbon structural steels*, .

27 E. Wakai, N. Okubo, M. Ando, T. Yamamoto and F. Takada, *Journal of Nuclear Materials*, 2010, 398, 64–67.

28 P. Layus, *Influence of alloying elements on the low-temperature properties of steel*, 2015.

29 J. Yu and C. J. Mcmahon, *I he ttects of Composition and Carbide Precipitation on Temper Embrittlement of Cr-1 Mo Steel Part I. Effects of P and Sn 2.25*, .

30 H. Qiu, T. Hanamura and S. Torizuka, *ISIJ International*, 2014, 54, 1958–1964.

31 M. Diez, A. Serani, E. F. Campana, F. Stern and E. F. Campana, DOI:10.48550/arXiv.2105.13062.

32 M. S. Bingley, *Effect of grain size and carbide thickness on impact transition temperature of low carbon structural steels*, .

33 K. Deb, A. Pratap, S. Agarwal and T. Meyarivan, *A Fast and Elitist Multiobjective Genetic Algorithm: NSGA-II*, 2002, vol. 6.

Snehungsu_M.Tech_MEMS_Thesis_Final_Print.pdf

ORIGINALITY REPORT

11%	9%	6%	5%
SIMILARITY INDEX	INTERNET SOURCES	PUBLICATIONS	STUDENT PAPERS

PRIMARY SOURCES

1	Submitted to Indian Institute of Management, Indore Student Paper	1%
2	Submitted to Indian Institute of Technology Indore Student Paper	1%
3	www.mdpi.com Internet Source	<1%
4	quieora.ink Internet Source	<1%
5	patents.justia.com Internet Source	<1%
6	link.springer.com Internet Source	<1%
7	Dexin Zhu, Kunming Pan, Hong-Hui Wu, Yuan Wu, Jie Xiong, Xu-Sheng Yang, Yongpeng Ren, Hua Yu, Shizhong Wei, Turab Lookman. "Identifying intrinsic factors for ductile-to-brittle transition temperatures in Fe–Al intermetallics via machine learning", Journal of Materials Research and Technology, 2023 Publication	<1%
8	arxiv.org Internet Source	<1%
9	Faridoddin Shariaty, Sanjiban Sekhar Roy. "MATLAB for Brain-Computer Interface Systems - Computation and Data Processing", CRC Press, 2025 Publication	<1%

10	Submitted to Birla Institute of Technology Student Paper	<1 %
11	Submitted to Swiss School of Business and Management - SSBM Student Paper	<1 %
12	phizze.com Internet Source	<1 %
13	worldwidescience.org Internet Source	<1 %
14	dokumen.pub Internet Source	<1 %
15	Ailong Fan, Yingqi Wang, Liu Yang, Xiaolong Tu, Jian Yang, Yaqing Shu. "Comprehensive evaluation of machine learning models for predicting ship energy consumption based on onboard sensor data", Ocean & Coastal Management, 2024 Publication	<1 %
16	ijred.cbiore.id Internet Source	<1 %
17	su.diva-portal.org Internet Source	<1 %
18	theses.gla.ac.uk Internet Source	<1 %
19	Submitted to Embry Riddle Aeronautical University Student Paper	<1 %
20	Tinkle Chugh, Yaochu Jin, Kaisa Miettinen, Jussi Hakanen, Karthik Sindhya. "A Surrogate-assisted Reference Vector Guided Evolutionary Algorithm for Computationally Expensive Many-objective Optimization", IEEE Transactions on Evolutionary Computation, 2016 Publication	<1 %

21	"Proceedings of the 13th International Conference on Metal Forming", steel research international, 09/2010 Publication	<1 %
22	Submitted to Interactive Design Institute Student Paper	<1 %
23	Thangaprakash Sengodan, Sanjay Misra, M Murugappan. "Advances in Electrical and Computer Technologies", CRC Press, 2025 Publication	<1 %
24	Submitted to University of Hertfordshire Student Paper	<1 %
25	Submitted to University of Teesside Student Paper	<1 %
26	css.jaist.ac.jp Internet Source	<1 %
27	www.frontiersin.org Internet Source	<1 %
28	Hongwei ZHENG, Tingdong LI, Rizheng HE, Haiying YU, Hui YANG, Yanlin WEN, Peng WANG, Fang LIU, Dongjun SUN. "P-wave Velocity Structure of Crustal and Upper Mantle beneath South China and its Tectonic Implications", Acta Geologica Sinica - English Edition, 2022 Publication	<1 %
29	assets-eu.researchsquare.com Internet Source	<1 %
30	D. S. Gelles. "Reduced activation ferritic alloys for fusion", Plasma Devices and Operations, 1994 Publication	<1 %
31	Seyedolmohadesin, Maedeh. "Neural Dynamics of Developmental Decision Making	<1 %

	and Sexually Dimorphic Behaviors in C. Elegans", Northeastern University, 2024 Publication	
32	dl-asminternational-org_proxy.dotlib.com.br Internet Source	<1 %
33	tudr.thapar.edu:8080 Internet Source	<1 %
34	www.science.gov Internet Source	<1 %
35	Hailong Cheng, Xinchun Luo, Xin Wu. "Recent research progress on additive manufacturing of high-strength low-alloy steels: Focusing on the processing parameters, microstructures and properties", Materials Today Communications, 2023 Publication	<1 %
36	Moitra, A., Arup Dasgupta, S. Sathyanarayanan, G. Sasikala, S.K. Albert, S. Saroja, A.K. Bhaduri, E. Rajendra Kumar, and T. Jayakumar. "A Study of Fracture Mechanisms in RAFM Steel in the Ductile to Brittle Transition Temperature Regime", Procedia Engineering, 2014. Publication	<1 %
37	apps.dtic.mil Internet Source	<1 %
38	backend.orbit.dtu.dk Internet Source	<1 %
39	discovery.researcher.life Internet Source	<1 %
40	elibrary.tucl.edu.np Internet Source	<1 %
41	jultika.oulu.fi Internet Source	<1 %
42	www.computersciencejournals.com Internet Source	

		<1%
43	www.researchgate.net Internet Source	<1%
44	Kim, Min-Chul, Ki-Hyoung Lee, Bong-Sang Lee, and Whung-Whoe Kim. "Mechanical Properties of SA508 Gr.4N Model Alloys as a High Strength RPV Steel", ASME 2010 Pressure Vessels and Piping Conference Volume 9, 2010. Publication	<1%
45	Lu Zhu, Bo Gao, Jun Wang, Runnong Chen, Yinpeng Wang, Chunhui Jiang, Yanguang Cao, Zhaodong Li. "Acquiring a low yield ratio well synchronized with enhanced low-temperature toughness in 550MPa grade bridge steels through intercritical quenching treatment", Journal of Materials Research and Technology, 2025 Publication	<1%
46	Shailesh Kumar Singh, Bashista Kumar Mahanta, Pankaj Rawat, Sanjeev Kumar. "Machine Learning-Assisted Design of High-Entropy Alloys for Optimal Strength and Ductility", Journal of Alloys and Compounds, 2024 Publication	<1%
47	Vivek Yadav, Deepanshu, Harshit Mittal, Vinay Shah, Omkar Singh Kushwaha. "Fuel Cell Degradation Prediction Using Machine Learning Models: A Study on Proton Exchange Membrane (PEM) Fuel Cell Dataset", Springer Science and Business Media LLC, 2025 Publication	<1%
48	archive.org Internet Source	<1%
49	ia601006.us.archive.org Internet Source	

		<1%
50	iccs.ac.in Internet Source	<1%
51	mirrors.aggregate.org Internet Source	<1%
52	researchcommons.waikato.ac.nz Internet Source	<1%
53	Muhammad Faizan Tahir, Muhammad Zain Yousaf, Anthony Tzes, Mohamed Shawky El Moursi, Tarek H.M. El-Fouly. "Enhanced solar photovoltaic power prediction using diverse machine learning algorithms with hyperparameter optimization", Renewable and Sustainable Energy Reviews, 2024 Publication	<1%
54	Junko Hutahaean, Vasily Demyanov, Mike Christie. "Many-objective optimization algorithm applied to history matching", 2016 IEEE Symposium Series on Computational Intelligence (SSCI), 2016 Publication	<1%
55	Wang, Xin. "Integrated Computational Materials Design for Alloy Additive Manufacturing: Introducing Data-Driven Approach to Physical Metallurgy.", University of Pittsburgh, 2024 Publication	<1%

Exclude quotes	On	Exclude matches	< 5 words
Exclude bibliography	On		